Biomass Refinery and Process Dynamics Thesis

Continuous optimization trajectories for energy efficient drying of broccoli with high levels of nutritional components

Rob van Olst

November 2013

WAGENINGEN UNIVERSITY
WAGENINGEN UR

Biomass Refinery and Process Dynamics Thesis

Continuous optimization trajectories for energy efficient drying of broccoli with high levels of nutritional components

Name	:	Rob van Olst
Registration number	:	881008-620-050
Program	:	Biosystems Engineering
Course code	:	BRD 80436
Number of Credits	:	36 ects
Examinators	:	dr. ir. A.J.B. van Boxtel dr. ir. L.G. van Willigenburg
Supervisor	:	dr. ir. A.J.B. van Boxtel
Period	:	2013
Chair Group	:	Biomass Refinery and Process Dynamics Bornse Weilanden 9 6708 WG Wageningen P: 0317- 482124

Pictures on the front page retrieved from: http://nl.123rf.com/photo_13778290_broccoli-op-een-witte-achtergrond.html

WAGENINGEN UNIVERSITY
WAGENINGEN UR

Summary

The research topic of this thesis is convective drying of broccoli using continuous optimal control strategies derived from dynamic optimization. Convective drying is the most applied approach to dry products, but it is also a process with a low thermal efficiency, as the efficiency is often below 60 %. Convective drying is also a major contributor to the industrial energy use in many countries.

When broccoli is dried, the nutritional content of the product will change due to the changing temperature and moisture content. Broccoli contains a relative high concentration of vitamin C and glucosinolates, which have a positive effect on human health. Glucosinolates and vitamin C are sensitive to heat and deteriorate during heat treatments such as drying. With this deterioration, the product quality will drop and the associated value of the product decreases. To prevent this deterioration, the product should be dried at low temperatures, but this decreases the energy efficiency of the drying process further.

To increase the efficiency of the drying process and to retain higher levels of vitamin C after drying, optimal drying trajectories were derived by using piecewise constant and piecewise linear functions in a previous study. The control variables that were considered were the temperature of the inlet air and the air flow rate. During this thesis the drying process of broccoli was optimized with continuous control trajectories instead of piecewise linear and constant functions and differences between the optimization techniques are indicated.

Before optimization was applied, the drying model used in the previous research was modified to prevent that air becomes saturated, as the saturated moisture content of the air was not limited to its physical boundaries, which resulted in a too large temperature drop due to evaporation of moisture. The modification did not have a significant effect on the vitamin C retention ratio, as the saturated moisture content of the air is only reached when the drying rate constant of vitamin C is still low. The modification resulted in a lower energy efficiency as the temperature drop was limited.

When only the inlet air temperature was used as a control variable, continuous optimization resulted in a vitamin C retention ratio of 38 % and an energy efficiency of 46 %, when drying for 10 hours and a final moisture content of 0.1 kg water / kg product. When the inlet air flow and temperature are controlled, the vitamin C retention ratio is 75 % and the energy efficiency 98 %. In both situations, better results are achieved in comparison to piecewise linear and constant functions.

To see the effect of a changing drying rate constant, a sensitivity analysis has been performed, where the drying rate was randomly changed 100 times around its nominal value with a standard deviation of 10 %. Results showed that the variation has little effect on the vitamin C retention ratio and the energy efficiency, but a large effect on the final product moisture content. New optimized control trajectories were calculated for a different initial product moisture content and a different drying rate constant. The found trajectories are compared with the nominal trajectories and differences are indicated.

Contents

1 Introduction

1.1 Background

The perception about food quality has changed during time. Environmental, health, and nutritional aspects have become more and more important (Verkerk *et al.* 2009). Quality attributes can be divided into intrinsic and extrinsic attributes. Intrinsic quality attributes are concerned with the product itself, while extrinsic quality attributes deal with the way the product is produced and processed. As intrinsic product qualities are becoming more and more important for consumers, a lot of research is done to increase and maintain intrinsic attributes of food, or keep losses as small as possible.

Convective drying is often used to preserve food products for a long period of time. With convective drying, a heated air flow is used to remove moisture from a product by vaporization. It is one of the oldest methods to preserve food products and the most applied technology (Kudra 2012), (Kemp 2005). Convective drying is an energy intensive process; it is estimated that for some industrial countries the energy consumption for drying can take up to 20 % of the total industrial energy demand (Kudra 2004). Although most of the heat from the fuel source is transferred to the drying air, the overall thermal efficiency of the drying process is often less than 50 % (Kemp 2005).

This thesis is focussing on the convective drying of broccoli. Broccoli is a vegetable that belongs to the group of *Brasicaceae.* Different studies identified that the consumption of vegetables from the group of *Brasicaceae* could help to reduce the risk of colon and rectal cancer (Voorrips *et al.* 2000). These properties are attributed to the high concentration of glucosinolates that are present in *Brasicaceae.* Broccoli also contains vitamin C, which is an antioxidant that could reduce the risk for cancer and heart diseases (Byers and Perry 1992; Byers and Guerrero 1995). Glucosinolates and vitamin C are sensitive to heat and they will degrade during heat treatments such as drying. With this degradation, the product quality will drop and the associated value of the product will decrease. To prevent this degradation, the product should be dried at low temperatures, but this will conflict with the economic and sustainability aims of the drying process, as a lower temperature results in a longer drying period and a decrease in the energy efficiency.

To increase the energy efficiency of the drying process and to retain higher levels of nutritional components after drying in comparison to a conventional convective drying process, optimal drying trajectories were derived by Jin (Jin *et al.* 2013) using piecewise constant and piecewise linear functions. The control variables that were considered were the inlet air temperature and the inlet air flow rate. The research showed that the best results were obtained using piecewise linear functions, with a vitamin C retention of 65 % and an energy efficiency of 55 %. These results were far better than when using a traditional constant setting of the controlled variables: 32 % retention for vitamin C and an energy efficiency of 28 %.

1.2 Problem statement

This thesis presents time continuous functions derived from dynamic optimization as an alternative for the piecewise linear and constant functions presented by Jin (Jin *et al.* 2013). In her implementation Jin used a simplified drying model where the saturated moisture content could exceed its maximum value, which resulted in an inaccuracy in the model outcomes. The saturated moisture content has to be limited to prevent unrealistic behaviour in the drying process.

The used models do not incorporate uncertainty. Most process models do not incorporate uncertainty and are a simplification of reality. An uncertain parameter in the drying model of

broccoli is the drying rate constant of broccoli stalks. Another uncertain parameter is the initial product moisture content. To see what the effect is of a changing drying rate constant and initial product moisture content, the parameter values are changed around its nominal value.

1.3 Thesis preview

The material and methods that have been used during this thesis will be presented in chapter 2. First the models will be presented that have been used to simulate the drying process, before discussing the used continuous optimization methods and the software that has been used to find an optimal solution. The results are presented in chapter 3. The result section starts with adaptations that have been made to the drying model, before presenting the results of continuous optimization. Afterwards the effects of uncertainty are presented, before showing the costate trajectories that are following from continuous optimization. The results will be discussed in chapter 4 and finally the reports ends with the conclusions in chapter 5.

2 Material and Methods

2.1 Problem formulation

This research only uses computer simulations to assess the performance of continuous optimization. To get a better understanding of the drying process, a schematic representation of a dryer is shown in Figure 1. At t = 0, broccoli is entering the dryer and it will stay here for 10 hours. After this period the moisture content of the product should have dropped from 9 kg water / kg product to 0.1 kg water / kg product. This process is controlled by varying the temperature (Tin) and flow of the air (Fa) that is entering the dryer. When the broccoli is dried, it is removed out of the dryer and a new batch can be dried.

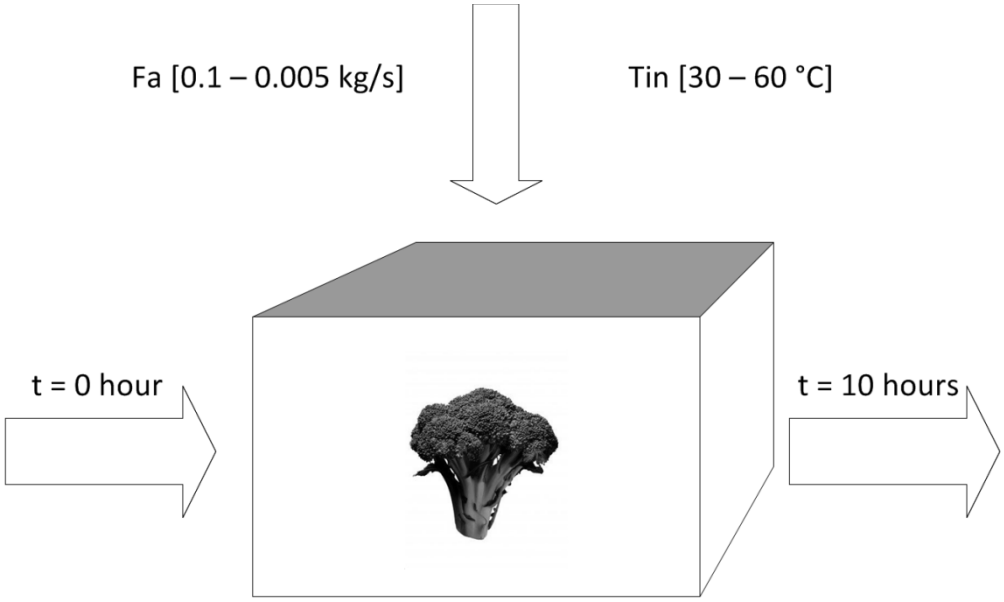

Figure 1: Schematic representation of the setup used for drying broccoli

To compare the results of this thesis with the work of Jin (Jin *et al.* 2013), the following optimization objectives and boundaries are used. The drying process is controlled by two control variables: the inlet air temperature and the inlet air flow rate. The control variables are constrained by:

$$30\,°C \leq T_{in} \leq 60\,°C \tag{1}$$

$$0.005\frac{kg}{s} \leq Fa \leq 0.1\frac{kg}{s} \tag{2}$$

These constraints are a consequence of the physical limitations of the dryer. The product temperature and the product moisture content affect the degradation rate constants of vitamin C and glucosinolates. Because the degradation rate constant of glucosinolates in this temperature range is very low, the minimization of the glucosinolates is not included in the objective function (see also Figure 2). This means that the cost function for this problem consists out of two parts: the minimization of the energy and vitamin C losses. The costs function J can be written as:

$$J = w_1\left(\frac{C}{C_0} - 1\right)^2 + w_2\left(\frac{\int_0^{tf}(\eta)dt}{tf} - 1\right)^2 \tag{3}$$

Where $\frac{C}{C_0}$ is the retention ratio of the vitamin C concentration compared to its initial concentration at the end of the drying process, η is the average energy efficiency at final time tf, and w_1 and w_2 are weight factors for the vitamin C retention and the energy efficiency. The retention ratio and the energy efficiency are both relative values and the aim is to bring them as close as possible to 1 at the end of the drying time. An advantage of the cost function formulation is that both terms have the same order of size which means that the errors are also in the same range and the optimization will affect both terms equally hard.

During the research the weight factors were set to 1, because both terms were in the same range and there was no preference for a higher vitamin C yield or a higher energy efficiency. The terms in the cost function are quadratic, which has two advantages over a non-quadratic formulation (van Willigenburg 2013). First of all large errors in the cost function will be better prevented by minimizing and secondly they are often easier and faster to compute, because quadratic functions and its integrals are smooth and often have a single global minimum.

The process is evaluated for a final drying time of 10 hours. At the end of the drying process the final moisture content in the broccoli has to be 0.1 kilogram of water per kilogram of product.

$$x(tf = 10) = 0.1 \ \frac{kg\ water}{kg\ product} \tag{4}$$

Simulations have been performed with only using the inlet air temperature as a control variable and keeping the air flow constant at 0.1 kg/s, and with the inlet air temperature and flow as control variables of the process.

2.2 Simulation models

Drying is a dynamic process during which the psychical properties of the product change. This paragraph discusses the models that are used to describe the drying behaviour of broccoli stalks and the degradation of its nutrients.

2.2.1 Drying models

The mass balance for the moisture content in the product during drying is given by:

$$\frac{dX}{dt} = -k(X - X_e) \tag{5}$$

With X being the moisture content (kg water.kg dry matter^{-1}) of the product, X_e is the equilibrium moisture content (kg water.kg dry matter^{-1}), k is the drying rate constant (s^{-1}).

Because analysis of experiments showed that the heating of broccoli stalks happens at a much faster time scale than the moisture transport during drying, it is assumed that the stalks and the air will have the same temperature in the dryer (Eisma 2010). This results in the following combined energy balance (Law and Mujumdar 2006):

$$M_p C_{pp} \frac{dT}{dt} = F_a\left(C_{pa} + X_{a,in} * C_{pv}\right)(T_{in} - T) \ldots \\ -F_a * \Delta H_{vap}\left(X_a - X_{a,in}\right) \tag{6}$$

$$X_a = \frac{M_p * \frac{dX}{dt} - F_a X_{a,in}}{-F_a} \tag{7}$$

Where F_a represents the air mass flow rate (kg. s^{-1} m^{-2}), X_a is the moisture content of the air (kg water.kg dry matter^{-1}), $X_{a,in}$ is the moisture content of the inlet air (kg water.kg dry matter^{-1}), and M_p is the dry weight of the product per m^2 floor surface area of the dryer. C_{pp} is the specific heat capacity of the product (kJ.kg^{-1}.K^{-1}), C_{pa} is the specific heat capacity of the air (kJ.kg^{-1}.K^{-1}), T is the product temperature and T_{in} the inlet air temperature (°C), and ΔH_{vap} the latent heat of vaporization (kJ.kg^{-1}).

The energy efficiency of the drying process follows from the following equation:

$$\eta(t) = \frac{T_{in}(t) - T_{air}(t)}{T_{in}(t) - T_{amb}} \quad (8)$$

Where η is the energy efficiency, T_{air} the air temperature (°C) and T_{amb} the ambient temperature (°C) outside the dryer. Because it is assumed that the air temperature is equal to the product temperature, equation (8) can also be written as:

$$\eta(t) = \frac{T_{in}(t) - T(t)}{T_{in}(t) - T_{amb}} \quad (9)$$

Table 1 shows the dryer characteristics that were used in this thesis.

Table 1: Dryer characteristics used for calculations and optimization

Parameter	Value
$\boldsymbol{M_p}$	$1\ [kg.m^{-2}]$
$\boldsymbol{T(t=0)}$	$25\ [°C]$
$\boldsymbol{C_{pa}}$	$1\ [kJ.kg^{-1}.K^1]$
$\boldsymbol{C_{pv}}$	$1.89\ [kJ.kg^{-1}.K^1]$
$\boldsymbol{C_{pp}}$	$0.837 + 1.256X\ [kJ.kg^{-1}.K^1]$ (Hussain and Dincer 2003)
$\boldsymbol{\Delta H_{vap}}$	$2500 - 2.386T[kJ.kg^{-1}]$ (Henderson-Sellers 1984)
$\boldsymbol{T_{amb}}$	$20\ [°C]$
$\boldsymbol{k}$	$0.22 \exp\left(-\frac{19403}{8.314T}\right)[s^{-1}]$
$\boldsymbol{X_{a,in}}$	$0.007\ [kg\ water.kg\ dry\ mater^{-1}]$
$\boldsymbol{X_e}$	$-\left(\frac{1}{5.18} * \log(1-H)\right) \exp\left(\frac{1}{0.93}\right)$ $[kg\ water.kg\ dry\ mater^{-1}]$ (Mulet *et al.* 1999)

2.2.2 Nutrient degradation models

The degradation model for vitamin C is based on experiments performed on different product samples (Mishkin *et al.* 1984; Karim and Adebowale 2009).

The degradation of vitamin C is described by a first order model using the following equations:

$$\frac{dC}{dt} = -k_c C \quad (10)$$

Where C is the concentration of vitamin C in the product (g.kg^{-1}), and k_c the degradation rate constant (s^{-1}). The temperature dependency for the degradation rate constant is given by:

$$k_c = k_{co} \exp\left(-\frac{E_{ca}}{RT}\right) \quad (11)$$

With R represents the gas constant (Cal.mol^{-1}.K^{-1}), E_a is the activation energy (Cal.mol^{-1}), and k_{co} the pre-exponential factor (min^{-1}). E_a and k_{co} are given by the following expressions:

$$k_{c0} = \exp(P_1 + P_2X + P_3X^2) \quad (12)$$

$$E_{ca} = P_4 + P_5X + P_6X^2 + P_7X^3 \quad (13)$$

The parameter values (P_1 - P_7) as used by Mishkin et al., are listed in Table 2.

Table 2: Vitamin C degradation kinetic model parameter values (Mishkin *et al.* 1984)

Parameter	Value
P_1	16.38
P_2	1.78
P_3	1.89
P_4	14831.00
P_5	241.10
P_6	656.20
P_7	236.80

Figure 2 shows a state diagram with contour lines for the degradation rate constants for vitamin C and glucosinolates. To reduce the vitamin C degradation, the temperature profile of broccoli should avoid crossing the contour lines. This figure shows why glucosinolates are not taken into consideration in the optimization process. The degradation of glucosinolates starts at a higher temperature and a lower moisture level in comparison with Vitamin C. Vitamin C degradation is not limited to within the contour lines. Also outside the contour lines degradation takes place, but the degradation rate constant will be low.

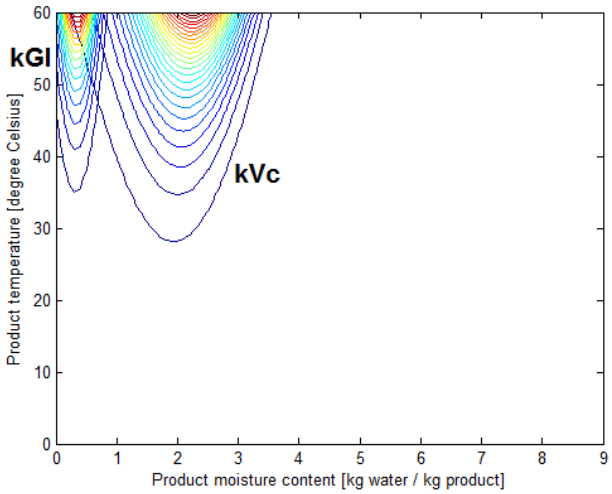

Figure 2: State diagram of fresh broccoli stalks with contour lines for the degradation rate constant of vitamin C (kVc) and glucosinolates (kGl)

A modification was made to the drying model to limit the saturated moisture content in the air. In the models and results presented by Jin (Jin *et al.* 2013) the moisture content of the air could exceed its natural saturation level. This can be explained with help of a Mollier-diagram (see Figure 3). The air coming into the dryer has a moisture content of 7 g water / kg dry matter. Point A in Figure 3 represents inlet air at 30 °C. The maximum moisture content of the air and the maximum temperature drop with an inlet temperature of 30 °C and a moisture content of 7 g water / kg dry matter, is reached at point B. During drying, the enthalpy in the air remains constant and the saturated moisture content of the air is reached when the relative humidity reaches 100 %. Without the modification, the model could for example reach point C,

which corresponds to an unrealistic high moisture content in the air and a temperature drop which is too large.

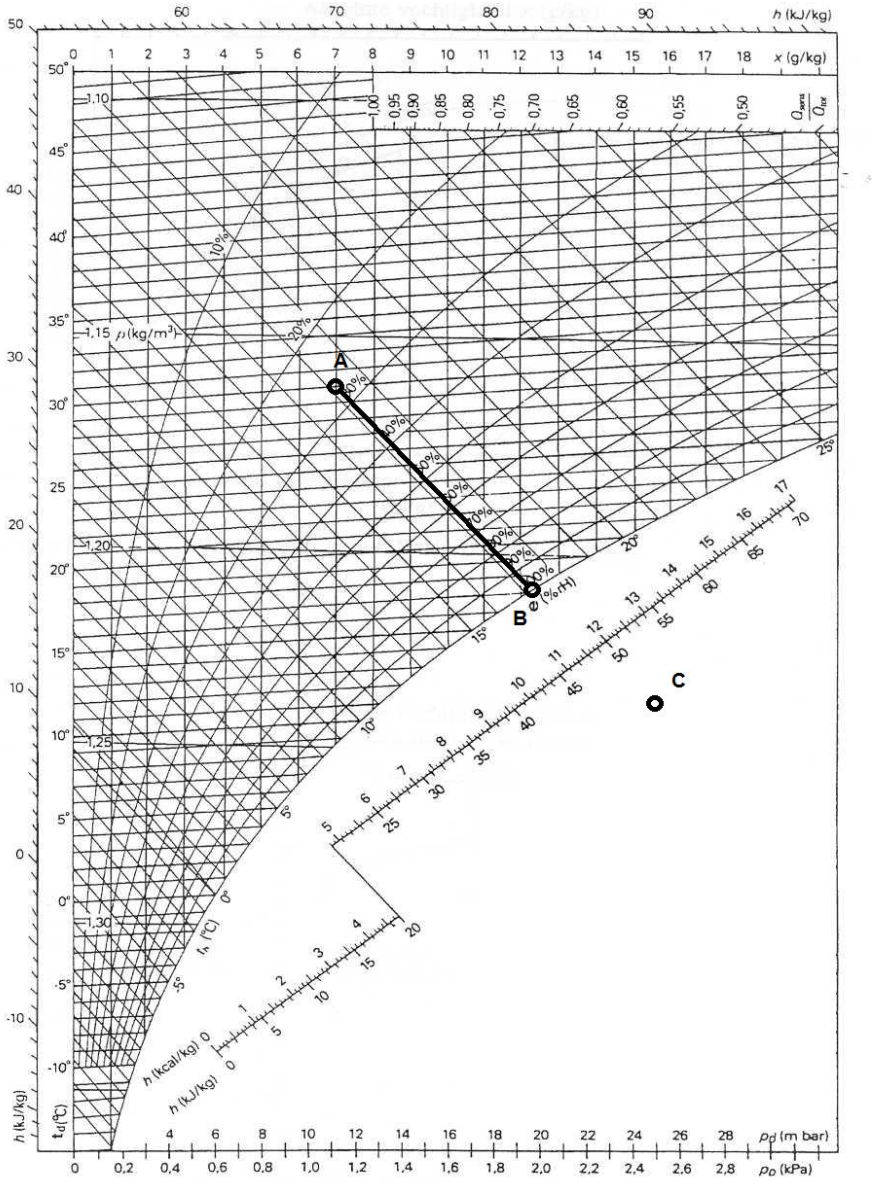

Figure 3: Mollier-diagram illustrating the maximum amount of moisture the air could contain and the maximum temperature drop that is possible when the product is dried (http://www.aspas.nl/).

The maximum moisture content of the air is restricted in this thesis to the saturated moisture content level. To see what the effect is of the adaptations to the drying model, the 4-stage piecewise linear optimization trajectories of Jin will be used in combination with the adapted model. Results will be compared with those obtained without the adaptations to the drying model.

To calculate the saturated moisture content of the air, an algebraic equation has been derived which can be solved using an equation solver in Matlab. However the equation solver has been replaced by a look-up table, because the use of the equation solver resulted in a big computational load and an increase in computation time. The saturated moisture content level is determined from the inlet air temperature and moisture content. The size of the temperature interval in the look-up table has a significant effect on the optimization process. When the

interval is chosen large the saturated moisture content value will also make large steps, which may result in sudden changes in the control variables. In reality the saturated moisture content of the air does not make steps, but it is a continuous function. So it makes sense to keep the temperature interval as small as possible. However, a small interval increases the computational load and the time to find an optimal solution. This means that a compromise has to be found: a high accuracy or a low computational load. In this thesis the temperature interval was set to 0.1 °C, which leads to an acceptable computational load and accuracy.

2.3 Continuous optimization

A common method to solve continuous optimization problems uses the Hamiltonian function, which was developed by Pontryagin (Pontryagin *et al.* 1962). To explain the method, a general optimal control problem will be formulated. Given the system (van Willigenburg 2013):

$$\dot{x} = f(x,u,t), \;\; x \in R^{n_x}, \; u \in R^{n_{xu}} \tag{14}$$

Where x represents the states of the system, u represents the control variables and the variable t time. The initial condition of the system is known:

$$x(t_0) = x_o \tag{15}$$

The optimized control variable u^* should be found that minimizes the cost function J:

$$J\big(u(t)\big) = \varphi(x(tf),tf) + \int_{t_0}^{tf} L(x,u,t)dt \tag{16}$$

φ represents the terminal costs and L the running costs, which are not present in the optimization problem of this thesis. Additional constraints on the final time may have to be satisfied as well:

$$\Psi(x(tf),tf) = 0, \;\; \Psi \in R^{n\Psi}, n_\Psi \leq n_x \tag{17}$$

For an optimum the following optimality equations should hold:

$$\dot{x} = \left(\frac{\partial H}{\partial \lambda}\right)^T = f, \;\; t_0 \leq t \leq t_f \tag{18}$$

$$-\dot{\lambda} = \left(\frac{\partial H}{\partial x}\right)^T = \left(\frac{\partial f}{\partial x}\right)^T \lambda + \left(\frac{\partial L}{\partial x}\right)^T, \text{ with } \lambda(tf) = \frac{\partial \varphi(tf)}{\partial x}, \; t_0 \leq t \leq t_f \tag{19}$$

$$0 = \left(\frac{\partial H}{\partial u}\right)^T = \left(\frac{\partial f}{\partial u}\right)^T \lambda + \left(\frac{\partial L}{\partial u}\right)^T, \;\; t_0 \leq t \leq t_f \tag{20}$$

Where H is the Hamiltonian and λ the Lagrange multiplier. Equation (18) is called the state equation, (19) is called the costate equation and (20) is the stationarity condition. The following boundary conditions are available:

$$x(t_0) \tag{21}$$

$$\Psi(x(tf),d(tf),tf) = 0, \quad if\ tf\ is\ fixed \tag{22}$$

$$\frac{\partial \varphi}{\partial x} + v^t \frac{\partial \Psi}{\partial x} - \lambda^T\Big|_{t=tf} = 0, \quad if\ tf\ is\ not\ entirely\ fixed \tag{23}$$

$$\frac{\partial \varphi}{\partial t} + v^t \frac{\partial \Psi}{\partial t} + H\Big|_{t=tf} = 0, \quad if\ tf\ is\ free \tag{24}$$

There exist two methods to solve a optimization problem by using the Hamiltonian functions: a direct and indirect search method (von Stryk and Bulirsch 1992). The direct search methods use the optimality equations above to solve the optimization problem. The initial conditions of

the Lagrange multiplier at $t = t_0$ should be known to calculate $\lambda(tf) = \frac{\partial \varphi(tf)}{\partial x}$. A solution can be found by changing u(t) such that the differential equations (14) are satisfied. Different methods exist to come to a solution. An advantage of the direct method is that you don't have to worry about the Lagrange multiplier. A disadvantage of direct methods is that they produce less accurate solutions than indirect methods, because the procedure is very sensitive for the initial values of λ. Another disadvantage is that there could be more local minima (von Stryk and Bulirsch 1992).

Indirect methods are based on Pontryagin's minimum (or maximum) principle. It uses the Hamiltonian optimality equations to solve the problem. Equation 18 represents n_x differential equations running forward in time and (19) represents n_x differential equations running backward in time. These equations are coupled by the stationarity condition in (20). Equation (21) represents n_x initial conditions and the boundary conditions provide n_x terminal conditions. This means that for each differential equation there is a single boundary condition available. Because these boundary conditions are specified at two time points, this problem is also known as a two point boundary value problem. The remaining n_x boundary conditions at $t = t_0$ and at $t = tf$ have to be found. Several methods are proposed to solve an optimal control problem by using the gradient $\frac{\partial H}{\partial u}$ (Bryson and Ho 1975; Bryson jr. 1999). A continuous variant is presented in the book of Bryson jr. (Bryson jr. 1999):

(a) guess u(t) for t = [0, tf];
(b) integrate forward $\dot{x} = f(x, u, t)$ with x(0) and u(t). Store x(t), u(t);
(c) evaluate φ, λ;
(d) integrate backward to compute $\frac{\partial H}{\partial u}$;
(e) calculate $\partial u = -k\frac{\partial H}{\partial u}$ and if ∂u < tolerance then stop;
(f) find new u(t); u(t) = u(t) + du(t), and;
(g) repeat (b) to (e).

The variable k represents the step size and it determines the number of iterations. An optimum is found when $\frac{\partial H}{\partial u} = 0$ or when it is smaller than the tolerance. This method by Bryson has been used to solve the optimal control problem.

The optimization problem was solved, using the same parameter values and conditions as presented by Jin (Jin *et al.* 2013) (see Table 1). The results are presented in state diagrams of product temperature against the product moisture content, as were used by Jin *et al.*

2.4 Software

To solve the optimization problems in this thesis, the continuous gradient method of Bryson has been implemented in the software package Matlab (Bryson jr. 1999). Matlab is a powerful tool to solve all kinds of mathematical problems. The software to solve the optimization problem can be divided into 4 sections:

- Initialization;
- Cost function;
- Process model, and;
- Optimization.

The main purposes of the initialization section is to determine the time span in which the optimization problem has to be solved, to present initial guesses for the control variables, and to give the initial values of the system states. In the cost function section, the cost function of the optimization problem is formulated and the terminal constraint is specified. The models that are used are specified in a separate file that contains all the information to simulate the problem. Finally the necessary steps for continuous gradient optimization, as presented in the

previous paragraph, are performed in the optimization section of the software. The Matlab code that has been used during this thesis can be found on the supporting cdrom.

2.5 Uncertainty in drying behaviour

2.5.1 Varying drying rate constant in combination with nominal control trajectories.

The drying rate constant contains some uncertainty, as it can vary for each batch that is dried. To see what the effect is of a changing drying rate constant, while still using the nominal control trajectories of the inlet air temperature and flow, a sensitivity analysis has been performed where the drying rate constant was randomly changed 100 times around its nominal value with a standard deviation of 10 %. Figure 4 shows the distribution in the samples. It can be seen that the samples approximate a normal distributed curve.

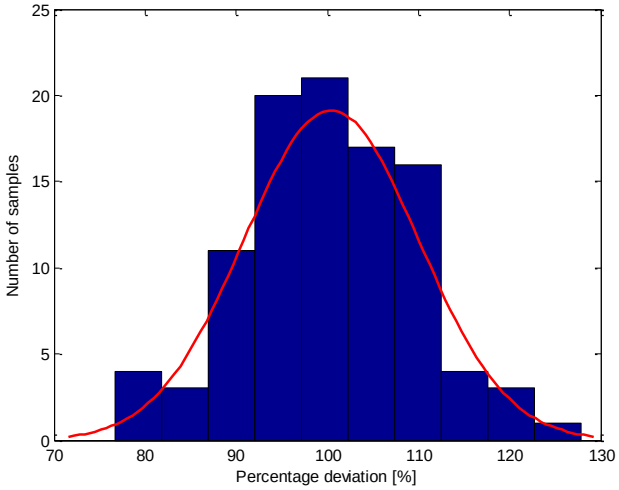

Figure 4: Histogram of 100 random chosen samples with a standard deviation of 10%, which are used to change the drying rate constant

2.5.2 Control trajectories when using a different drying rate constant and initial product moisture content

During another experiment, the drying rate was changed to 110 % of its nominal value, and the optimization was performed again. This resulted in different control trajectories in comparison the nominal trajectory. The same procedure was repeated while the initial product moisture content was changed to 90 % and 110 % of its nominal value. The results will be showed in the next chapter.

2.6 Costates

As is stated by (19), the costate equation is the negative first derivative of the Lagrange multiplier is equal to the partial derivatives of the Hamiltonian with respect to the state variables. The optimal costate $\lambda^*(t),\ t_0 \leq t \leq t_f$ represents the so called marginal costs. The costate equation can also be rewritten as:

$$-\lambda^{*T}(t) = \frac{\partial J^*(t,t_f)}{\partial x^*(t)} \leftrightarrow -\lambda_i{}^*(t) = \frac{\partial J^*(t,t_f)}{\partial x_i{}^*(t)}, i = 1,2,\dots, t_0 \leq t \leq t_f \qquad (25)$$

In this equation $J^*(t,t_f)$ are the minimum costs made from t to t_f when the state at time t is $x^*(t)$ (van Willigenburg 2013). This means that during the whole time interval $t_0 \leq t \leq t_f$, $-\lambda_i{}^*(t)$ represents the sensitivity of the minimum costs $J^*(t,t_f)$ to a change of the state variable $x_i{}^*(t)$.

The optimization problem in this thesis has three constraints: the vitamin C retention ratio (3), the energy efficiency (3) and the product moisture content (4). This report shows the costate trajectories of the product moisture content as state variable and the three constraints. The trajectories are explained by evaluating the state and control trajectories.

3 Results

3.1 Adaptations to the drying model

The drying model as presented by Jin (Jin *et al.* 2013) has been adapted to correct the saturated moisture content in the air. To see what the effect is of this adjustment, the control trajectories created by Jin using 4-stage piecewise linear functions and controlling the air temperature and flow, were used in combination with the adjusted drying model. The differences between the two models are shown in Figure 5. The first difference that can be seen is the temperature drop in the beginning of the drying process. With the non-adjusted drying model the temperature drops below 15 °C, which should not be possible with a minimum inlet temperature of 30 °C and an inlet moisture content of 0.007 kg water/kg dry matter. With the adjusted model the temperature only drops just below 20 °C at the beginning of the drying process. The temperature difference between the two trajectories has no effect on the vitamin C retention ratio, because the product moisture content is still high and the product temperature low, so the degradation rate is small. The difference does have an effect on the on the energy efficiency of the process. According to8, the lower the air temperature in comparison to the ambient temperature of 20 °C, the higher the energy efficiency will be. Table 3 shows that with the non-corrected drying model a higher energy efficiency is obtained in both control situations. The difference is only small, because the moisture content of the air is only for a short period of time at its saturation value, as drying goes fast at the beginning of the drying process. Piecewise linear controls are only used to indicate the effect of the adjusted drying model. All further simulations and figures are based on continuous optimization.

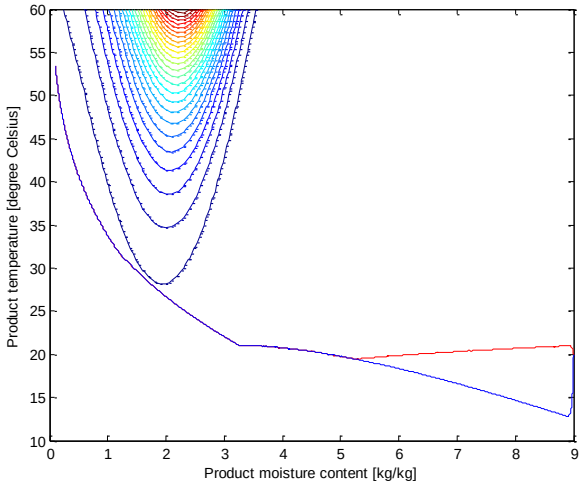

Figure 5: 4-stage piecewise linear controlled air temperature and flow trajectories. The red trajectory incorporates the adjusted drying model, whereas the blue trajectory does not.

Table 3: Vitamin C retention, energy efficiency, and product moisture content after drying when using two different drying models

	Controlling air temperature		Controlling air temperature and flow	
	Original drying model	Corrected drying model	Original drying model	Corrected drying model
Vitamin C retention [%]	35	35	45	45
Energy efficiency [%]	47	41	48	46
Moisture [kg water / kg product]	0.1	0.1	0.1	0.1

3.2 Continuous control trajectories of the broccoli drying process

3.2.1 Controlling the inlet air temperature

When using the inlet air temperature as a control variable and a constant inlet air flow of 0.1 kg/s, different results were obtained with continuous dynamic optimization in comparison to piecewise linear optimization. After a drying period of 10 hours the moisture content of the broccoli stalks was reduced from 9 kg water / kg product to 0.1 kg water / kg product with an energy efficiency of 46 % and a vitamin C retention of 38 %. Piecewise linear optimization reached the moisture reduction with an energy efficiency of 35 % and a vitamin C retention of 41 % when using 4-stage piecewise linear functions. Figure 6 shows the control trajectory which was obtained with continuous optimization. The inlet air temperature is at its lower bound to minimize the vitamin C degradation at the beginning of the drying process. To realize the final moisture content of 0.1 kg water / kg product, the air temperature of increases after 5 hours. To achieve this constraint the inlet temperature starts to increase. In Figure 7 it looks like the vitamin C degradation area is avoided, but as mentioned before, the degradation is not restricted to the contour lines.

Figure 7 shows that the product temperature drops below the ambient temperature of 20 °C at the beginning of the drying process. This drop is caused by the evaporation of moisture out of the product. The necessary energy that is needed to evaporate the moisture is partly provided by the temperature drop. The maximum temperature drop is limited by the amount of moisture the air can take up at a certain temperature. Equation (8) shows that the energy efficiency exceeds 100 % when the air temperature is lower than the ambient temperature. From an energy efficiency point of view this is a preferred situation. An energy efficiency higher than 100 % may sound a bit unnatural, but the “external” energy is provided by the relative high ambient temperature of 20 °C.

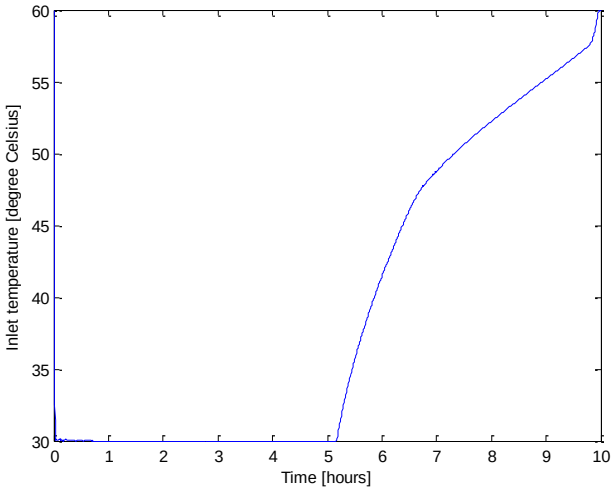

Figure 6: Inlet air temperature trajectory using continuous optimization and a drying time of 10 hours

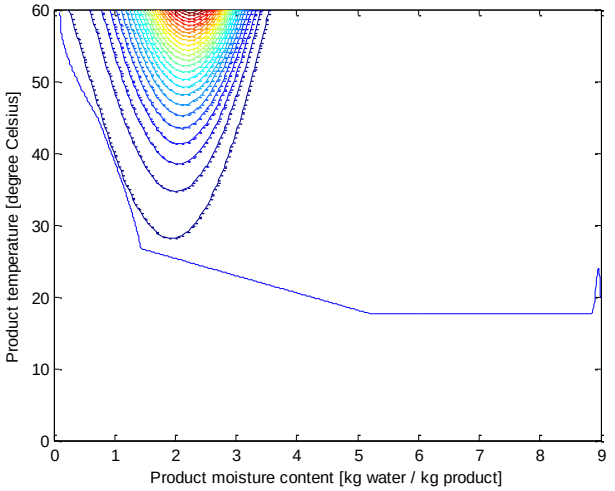

Figure 7: Product temperature trajectory in the state diagram with a continuous controlled air temperature and a drying time of 10 hours

3.2.2 Controlling the inlet air temperature and flow

Figure 8 and Figure 9 show the control trajectories of the inlet air temperature and flow. In comparison to the situation where only the input temperature is controlled, the vitamin C retention changed to 75 % and the energy efficiency to 98 %, while drying the product to 0.1 kg water / kg product in 10 hours. Piecewise linear optimization only reached a vitamin C retention ratio of 45 % and an energy efficiency of 46 %. At the beginning of the process the inlet temperature is around 30 °C and the air inlet flow is around 0.005 kg/s. Because of the low inlet air temperature and flow, the air temperature remains below the ambient temperature of 20 °C for a long period of time (see Figure 10). After six hours of drying the inlet air temperature starts to increase to reach the final product moisture content of 0.1 kg water / kg product. Because the product moisture content and temperature are low, the vitamin C degradation area is avoided almost completely. In Figure 10 it seems that the degradation contour lines are avoided completely, but the degradation area is bigger than represented by the contour lines. Because the air temperature is below the ambient temperature of 20 °C the

energy efficiency is maximized as explained earlier in this chapter and an efficiency of >100 % is obtained during some periods of time.

The air flow trajectory shows a slight increase at the beginning of the drying process. The increase is only small (10 % of its lower minimal value), and the influence on the drying process is little. Figure 11 shows the decrease in product moisture content during the drying process. It shows that at the beginning of the drying process the evaporation of moisture out of the product is higher than at the end of the drying process.

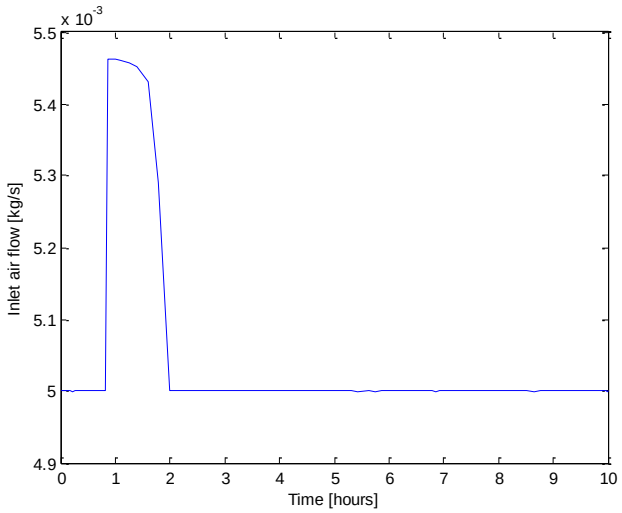

Figure 8: Control trajectory of inlet air flow during drying process

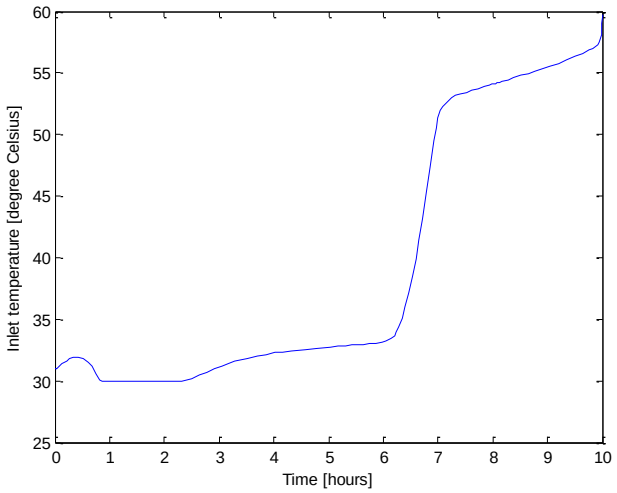

Figure 9: Control trajectory of inlet air temperature during drying process

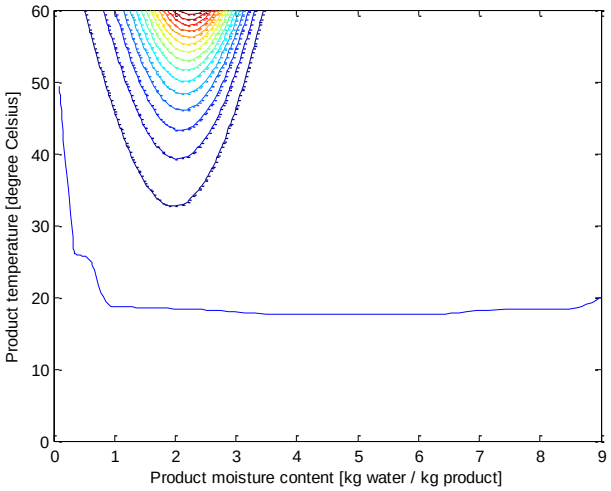

Figure 10: Product temperature trajectory against the product moisture content when controlling the inlet air temperature and flow

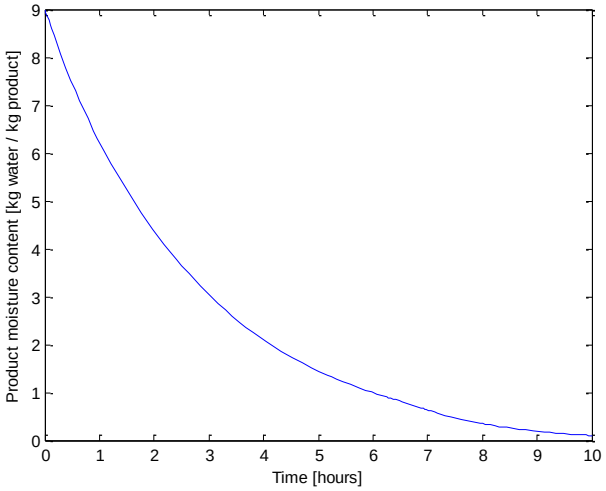

Figure 11: Product moisture content trajectory, when controlling the inlet air temperature and flow

The results can be compared in to two ways with the results of piecewise linear optimization. First of all, the final moisture content, vitamin C retention and energy efficiency can be compared. Another possibility is to compare the final costs after optimization. The lower the final costs, the better the optimization algorithm succeeded to optimize the process.

Table 4: Costs after optimization

	Controlling inlet air temperature	**Controlling inlet air temperature and flow**
Jin (piecewise linear)	0.771	0.594
van Olst (continuous)	0.709	0.075

Table 4 shows that continuous optimization resulted in an improvement in comparison to piecewise linear optimization, as in both control situations the cost are lower with continuous optimization. Especially when the inlet air temperature and flow are controlled, continuous

optimization results in lower costs after drying in comparison to 4-stage piecewise linear functions.

3.3 Uncertain drying rate constant

The results for variations in the drying rate constant are presented in Figure 12, Figure 13, and Figure 14, which show the results when the drying rate constant is randomly changed 100 times with a standard deviation of 10 %. The figures show that a varying drying rate has little effect on the vitamin C retention ratio at the end of the drying process, but that the vitamin C degradation can follow different trajectories. When the drying rate constant is larger than nominal, the degradation sets in earlier, as the degradation area is reached sooner. When the degradation peak is passed, the degradation rate decreases, as the distance between the product temperature state diagram and the degradation area becomes larger. At the end of the drying process, the degradation rate increases, as the distance becomes smaller again. When the drying rate constant is small, the degradation area is reached further in the drying process. Because the drying rate is small, it takes more time to pass the degradation area. As a consequence the degradation rate remains high for a longer period, resulting in a vitamin C retention ratio, which is almost the same with a high drying rate constant.

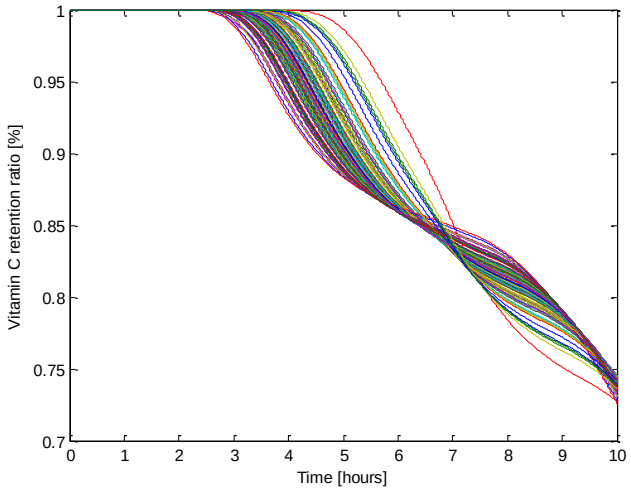

Figure 12: Vitamin C degradation trajectories as function of time obtained with optimized continuous control trajectories for the inlet air temperature and flow. The drying rate constant was randomly changed 100 times around its nominal value with a standard deviation of 10 %

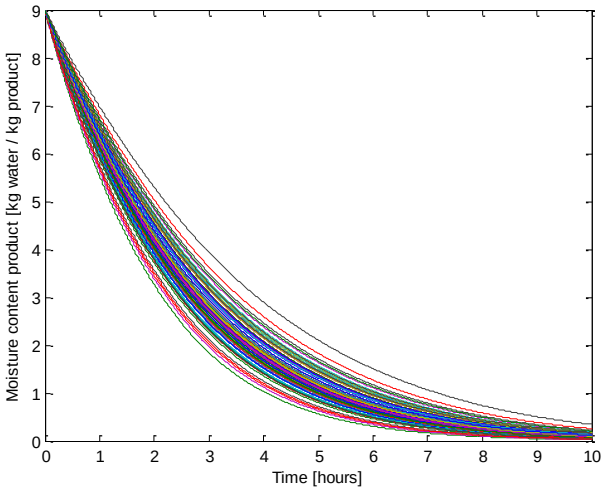

Figure 13: Product moisture content trajectories as function of time obtained with optimized continuous control trajectories for the inlet air temperature and flow. The drying rate constant was randomly changed 100 times around its nominal value with a standard deviation of 100 %

Figure 13 shows the product moisture content as function of time. It shows that not all trajectories reach the desired final moisture content of 0.1 kg water / kg product. When the drying rate constant is smaller than nominal, the final moisture content is higher in comparison to the nominal trajectory. When the drying rate constant is bigger than nominal the final moisture content will be lower than nominal. This implicates that the drying process could stop earlier and a higher vitamin C retention ration is achieved.

Figure 14 shows that the product temperature state diagrams for the different drying rates show the same trend. Some lines stop earlier than others, because they don't reach the desired final moisture content of 0.1 kg water / kg product. Although the same control trajectories were used to obtain the 100 simulations, the product temperature trajectories differ. This difference is explained by the different product moisture trajectories, because a different product moisture content trajectory results in a different air moisture content trajectory. The moisture content in the air will affect the amount of water that can evaporate out of the product, and as a consequence the temperature drop of the product due to evaporation.

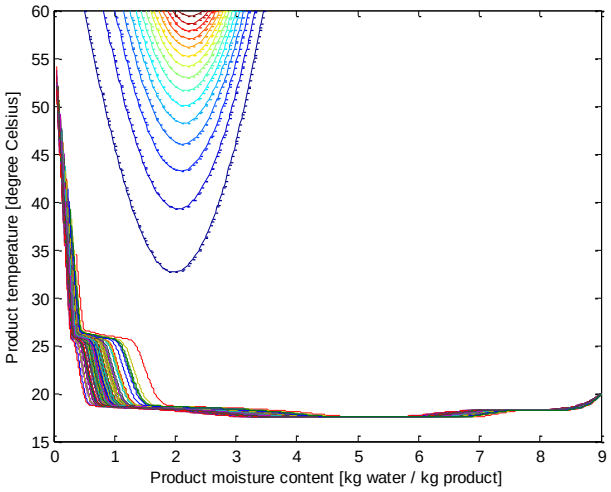

Figure 14: Product temperature trajectories as function of the product moisture content obtained with optimized continuous control trajectories for the inlet air temperature and flow. The drying rate constant was randomly changed 100 times around its nominal value with a standard deviation of 100 %

Table 5 shows the results of the 100 simulations with a randomly chosen drying rate constant and a standard deviation of 10 %. As earlier seen in the figures, a varying drying rate constant has little effect on the vitamin C retention. The effect on the energy efficiency is already a bit bigger, but a varying drying rate constant has especially an effect on the product moisture content.

Table 5: Drying result when randomly changing the drying rate constant 100 times with a standard deviation of 10%

	Mean	Standard deviation
Moisture content [kg water / kg product]	0.1074	0.0532
Vitamin C retention [%]	73.96	0.63
Energy efficiency [%]	98.13	2.40

3.4 Effect of step size in look-up table

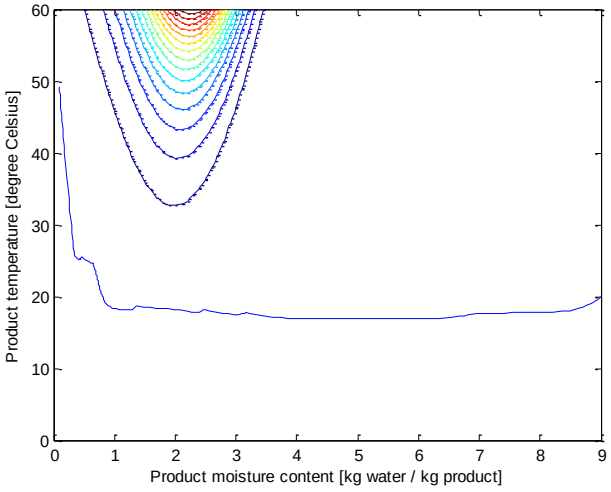

Figure 15: Product temperature trajectory as function of the moisture content in the product when controlling the inlet air temperature and flow

Figure 15 shows the product temperature as function of the moisture content when the inlet air flow and temperature are optimized using continuous optimal control. The saturated moisture content of the air is adjusted with a look-up table with a temperature interval of 1 °C. This means for example that when the inlet temperature is in the range 35 °C to 36 °C the saturated moisture content belonging to 35.5 °C is assigned. This method has been chosen, because solving the algebraic equation for the saturated moisture content during optimization resulted in a large computational load, which slowed down the optimization process dramatically. By using a look-up table, this problem has been overcome. The optimization settings are equal to those in the previous paragraph. Figure 15 clearly shows a different trajectory in comparison to Figure 10. The results obtained in Figure 10 were obtained with a temperature step of 0.1 °C, which resulted in a much smoother trajectory. Figure 15 shows some ripples on the trajectory which are caused by a change in the assigned saturated moisture content of the air. Because the temperature step is relatively large at 1 °C, the saturated moisture content makes also a big step. The ripples can be reduced by making the temperature step smaller. During all other simulations in this thesis, a temperature step 0.1 °C was used.

3.5 Costate trajectories

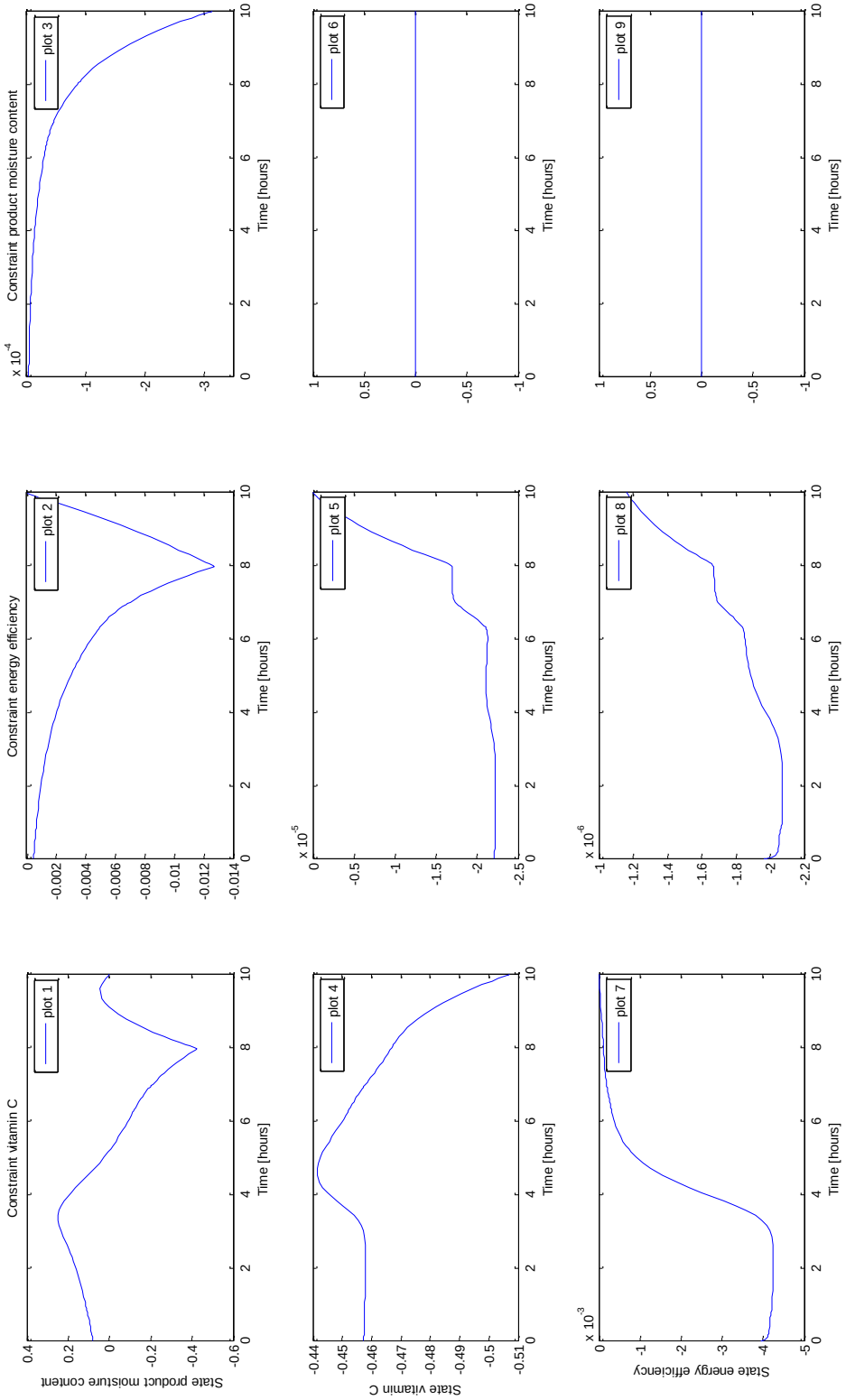

Figure 16: Costate trajectories, with the vitamin C retention ratio, the energy efficiency, and the product moisture content as state variables, when using nominal control trajectories.

Figure 16 shows nine costate trajectories, which show the sensitivity of changes in the state variables; vitamin C retention ratio, energy efficiency, and product moisture content, on the constraints of the optimization problem. The costate trajectories show some remarkable

events. The first row shows the effect of the vitamin C state variable. The first plot shows that the costate is increasing, until a maximum is reached after 3.5 hours. At this point (A in Figure 17) the maximum degradation rate is reached, and the distance between the product temperature and the vitamin C degradation area in the temperature/moisture state diagram is minimal (see Figure 10). From this point, the sensitivity starts to decrease again, as the distance to the degradation area starts to increase again. After 8 hours (B in Figure 17) the product temperature starts to increase rapidly to reach the desired final product moisture content (see Figure 19). This results in an increase of the vitamin C degradation rate again, and an increase of the costate value.

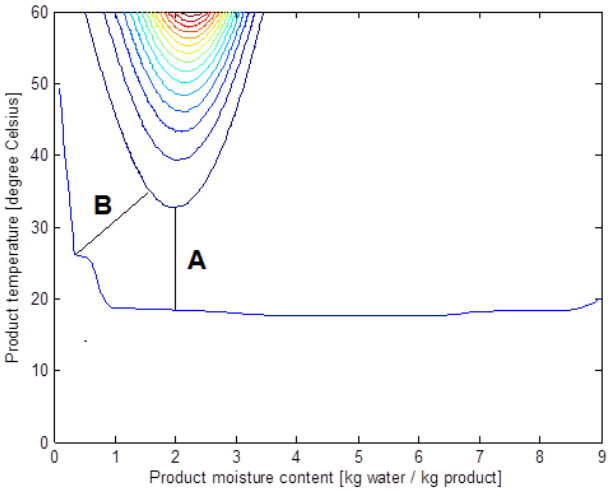

Figure 17: Product temperature trajectory as function of the moisture content in the product when controlling the inlet air temperature and flow

Plot 2 shows that the sensitivity is decreasing till 8 hours, when looking to the energy efficiency constraint. As in the previous plot, the temperature starts to increase rapidly from this point. No clear explanation is found, why this increase in product temperature leads to a sudden change in the costate trajectory. Plot 3 shows that the sensitivity of the product moisture content decreases as the final moisture content is nearing. At the end of the process the sensitivity decreases faster, as a change of the state variable with one unit, will have relative larger effect on the constraint. Plots 6 and 9 show that the other states do not have an effect on the product moisture content constraint. To reach a final product moisture content level of 0.1 kg water/ kg product, only the product moisture content state has an influence.

Plots 4 and 7 show that the vitamin C and energy efficiency state variables have little effect on the vitamin C constraint until 3 hours. At this point the vitamin C starts to degrade, as shown in Figure 18. The maximum degradation rate is reached just after 4 hours. In plot 4 this point corresponds to the maximum in the costate trajectory and in plot 7 this point is corresponds to the point of inflection in the costate trajectory. After the maximum degradation rate is reached, the costate sensitivities change. Plots 4 and 7 do not show a clear point after 8 hours, which marks the decrease of the drying rate constant, as can be seen in plots 1 and 2.

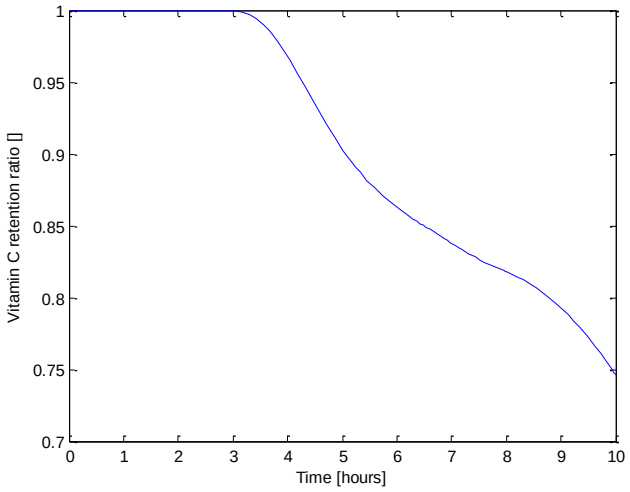

Figure 18: Vitamin C degradation rate, when using nominal control trajectories for the inlet air temperature and flow

Plots 5 and 8 follow almost the same trajectory as the product temperature as shown in Figure 18. This indicates that the product temperature plays an important role in determining the energy efficiency. This corresponds to equation (8), where the energy efficiency is calculated based on the inlet, air, and ambient temperature.

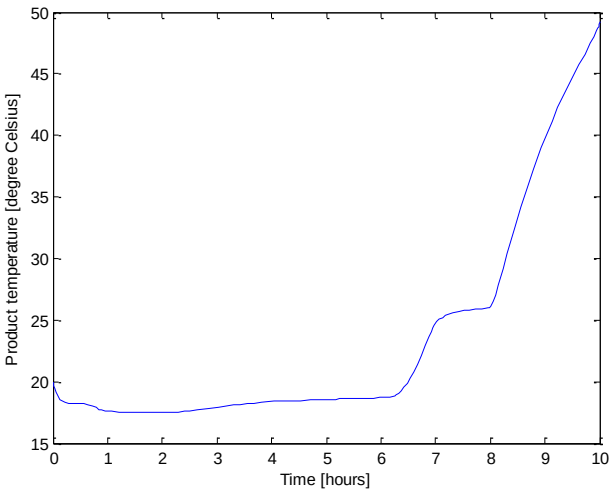

Figure 19: Product temperature trajectory, when using nominal control trajectories for the inlet air temperature and flow

3.6 Optimization trajectories for a different initial product moisture content and drying rate constant

In the previous paragraph, the effect of the drying rate constant was investigated. The variable was randomly changed 100 times with a standard variation of 10 % of its nominal value. To see how a deviation in the drying rate affects the optimization process, continuous optimal control trajectories have been calculated for a drying rate constant which is 10 % higher than nominal. Figure 20 and Figure 21 show the control variable trajectories for the adjusted drying rate constant, and Figure 22 shows the state diagram of the product temperature.

Just as with the nominal trajectory the inlet air flow shows a slight increase at the beginning of the drying process when the drying rate constant is increased. The increase is not has high in comparison to the nominal trajectory, but it continues for a longer period. Because the drying rate constant is higher, moisture will evaporate faster out of the product. As a consequence, the inlet air temperature will be lower, as less effort has to be done to reach the desired product moisture content of 0.1 kg water / kg product. The inlet air temperature also starts to increase sooner when the drying rate constant is higher. Because the moisture will evaporate faster, the vitamin C degradation area is reached sooner. The state diagram of the product temperature shows that both trajectories show the same trend. At the beginning of the drying process, the moisture content of the air is at its saturation value, causing a temperature drop in the product. As a consequence the product temperature remains low, and the vitamin C degradation rate is minimal. At the end of the drying process, the temperature of the nominal trajectory starts to increase a bit sooner to reach the desired product moisture content. Because the trajectories do not differ much, the final vitamin C retention ratio and energy efficiency are in the same range. When the drying rate constant is increased the vitamin C retention ratio reaches 74 % and the energy efficiency 98 %.

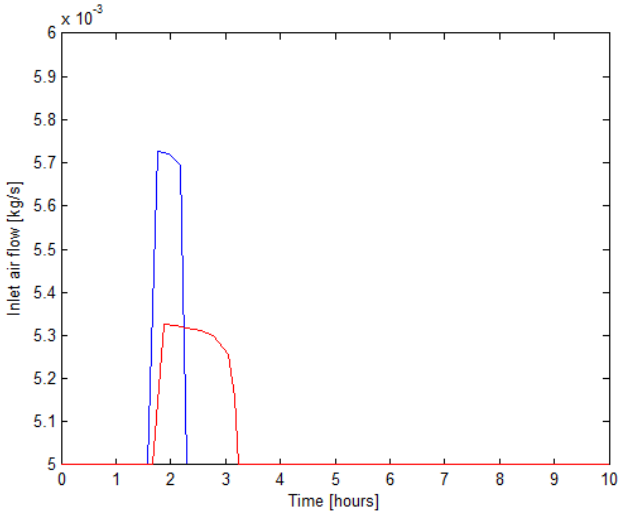

Figure 20: Inlet air flow trajectory for a nominal (blue), and a 10 % higher than nominal (red) drying rate constant.

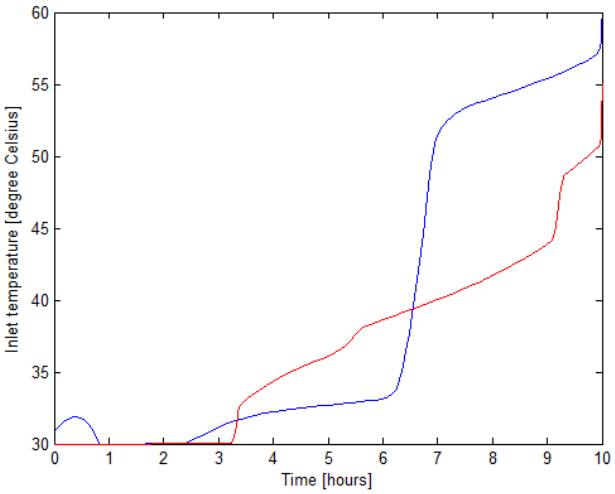

Figure 21: Inlet air temperature trajectory for a nominal (blue), and a 10 % higher than nominal (red) drying rate constant.

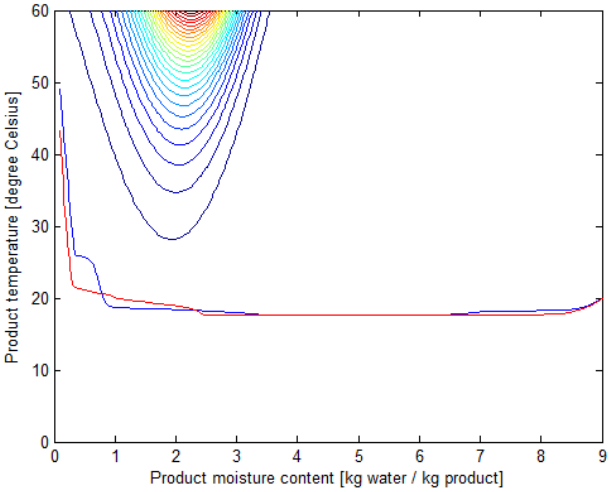

Figure 22: Product temperature trajectory in a state diagram for a nominal (blue), and a 10 % higher than nominal (red) drying rate constant.

Another variation was applied on the initial product moisture content. During the simulations, the nominal product moisture content was 9 kg water / kg product. To see what the effect is of a varying product moisture content, its value was changed to + 10 % and – 10 % its nominal value. In both situations a final product moisture content of 0.1 kg water / kg product is reached, with a vitamin C retention ratio of 75 % and a energy efficiency of 98 %. Figure 23 shows the inlet air temperature trajectories. At the beginning of the drying process the inlet air temperature is higher for a longer period, when the product moisture content is higher than nominal. After one hour the trajectories are similar, but after about 6.5 hours the the trajectory belonging to the higher initial product moisture content will reach higher temperatures. These higher temperatures are necessary to evaporate the extra moisture that is present in the product. Figure 24 shows the inlet air flow trajectories. During most of the time, the trajectories are at the lowest air flow rate. At the beginning of the drying process, some defined peaks can be seen. These peaks occur at time instances when the inlet air temperature is reaching or leaving its minimum temperature (see Figure 23). These peaks are probably caused by numerical problems in the optimization algorithm.

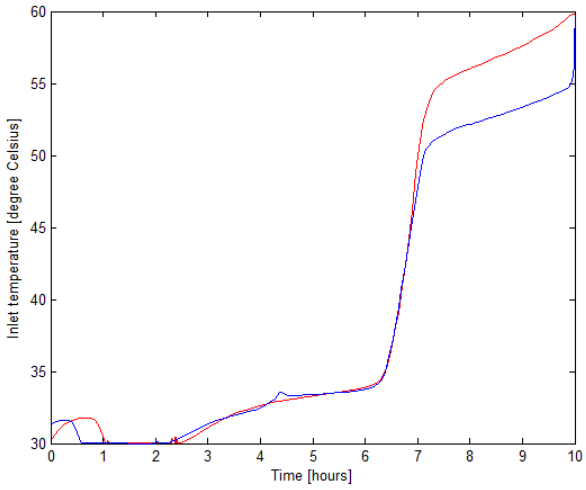

Figure 23: Inlet air temperature trajectories with different initial product moisture content. The red trajectory belongs to an initial product moisture content of + 10 % of the

nominal value and the blue trajectory belongs to an initial product moisture content of – 10 % of the nominal value.

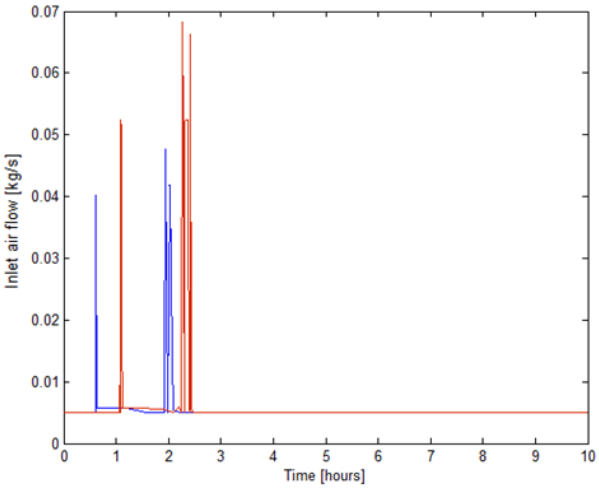

Figure 24: Inlet air flow trajectories. The red trajectory belongs to an initial product moisture content of + 10 % of the nominal value, and the blue trajectory belongs to an initial product moisture content of – 10 % of the nominal value.

Figure 25 and Figure 26 show the product temperature profiles against time and product moisture content. The trajectories with a different initial product moisture content are quiet similar, where a higher product temperature is reached when the initial moisture content is higher. The higher temperature at the end is necessary to evaporate the extra moisture in the product. Because the product temperature trajectories are similar, the vitamin C retention ratios at the end of the drying process and the energy efficiency are almost equal to the nominal case.

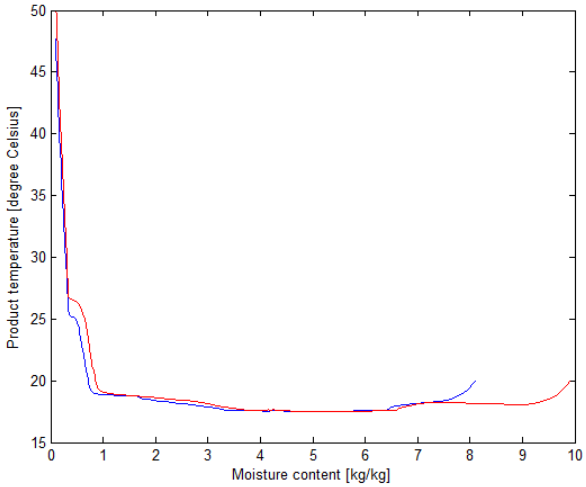

Figure 25: Product temperature trajectories, while the product moisture content changes. The red trajectory belongs to an initial product moisture content of + 10 % of the nominal value, and the blue trajectory belongs to an initial product moisture content of – 10 % of the nominal value.

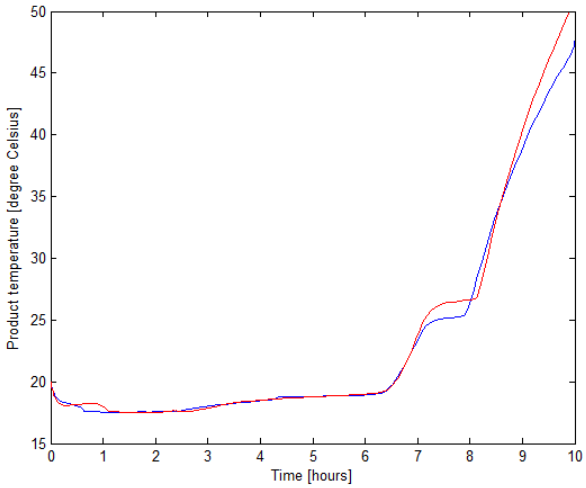

Figure 26: Product temperature trajectories over time. The red trajectory belongs to an initial product moisture content of + 10 % of the nominal value, and the blue trajectory belongs to an initial product moisture content of – 10 % of the nominal value.

4 Discussion

When the results of continuous optimization are compared with 4-stage piecewise linear optimization, different results are found. There are three explanations for these differences. First of all, continuous optimization is more "flexible" in comparison to piecewise linear optimization. With piecewise linear optimization there are only a limited number of possibilities to change the control variables, as with continuous optimization the control variables can be changed at every time instance. This flexibility increases the possibilities to avoid the vitamin C degradation area and to keep the energy efficiency high.

The second reason is that a different method has been used to calculate the energy efficiency of the drying process. Jin calculated the energy efficiency by using (5) at every time instance the optimization algorithm produced an answer, after which she took the average value as the energy efficiency of the system. This method does not take into account the different time intervals during simulation of the optimization algorithm, which means that every answer is given the same importance. This research used a different approach to overcome this problem. The integral of the energy efficiency over time is calculated and divided by time, which results in the average energy efficiency, while incorporating the different time intervals in between the answers of the optimization algorithm. The third reason for the difference between the answers has to do with the modification to the drying model. Table 3 showed that the non-adjusted drying model resulted in a too high energy efficiency, because the saturated moisture content of the air was not limited.

In her paper, Jin presented different results while using 4-stage piecewise linear optimization in comparison to the results obtained with 4-stage piecewise linear optimization in this report. Her research showed that the best results were obtained using 4-stage piecewise linear functions, with a vitamin C retention of 65 % and an energy efficiency of 55 %, when controlling the inlet air temperature and flow. During this thesis a vitamin C retention ratio of 45 % and an energy efficiency of 48 % was achieved, when using piecewise linear functions. Explanations for the different energy efficiencies where already given. There are two possible reasons which explain the differences in the vitamin C retention ratio after drying. First of all it was not exactly known which settings of the optimization algorithm Jin used. It could be that she used different settings of the algorithm, which resulted in a different (local) optimum. The second reason is that Jin might have used a different vitamin C degradation model in her paper. Figure 27 shows the contour lines for the degradation rate constant of vitamin C and glucosinolates as presented by Jin (Jin *et al.* 2013) (light blue lines), and the contour lines for the degradation rate constant of vitamin C as used in this report (coloured lines). Although the contour lines do not represent the same degradation rate constant, slightly different trajectories are shown. This indicates that possible a different kinetic model has been used.

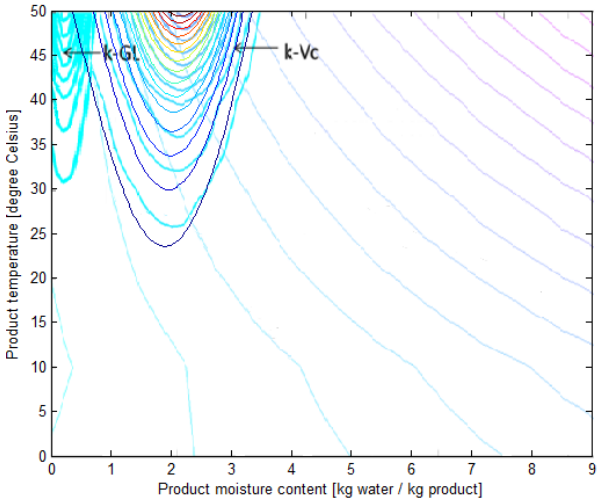

Figure 27: Contour lines for the degradation rate constant of vitamin C (k-Vc) and glucosinolates (k-Gl). The light blue lines correspond to the model used by Jin (Jin *et al.* 2013), and the coloured lines correspond to the degradation kinetic model used in this report.

In the optimized continuous control trajectory of Figure 24, some clear peaks can be seen. These peaks are caused by the use of a look-up table. These peaks are not desired and realistic when the control trajectories are transferred to a convective drying oven. The oven cannot realize such rapid changes in the product temperature. To overcome this problem the peaks should be filtered out of the control trajectories before implemented on an oven.

The continuous optimization algorithm of Bryson (Bryson jr. 1999) that has been used in this report needs initial guesses of the system states and the control variables as inputs besides the step size k and the number of iterations. These values should be chosen carefully, because they affect the optimization process. If the step size is chosen in the wrong range, the optimization may not reach an optimum, because it will not converge to an optimum. The best way to find a suitable step size is by trying different values and to see how they affect the costs after optimization. The same holds for the number of iterations. By trial and error a reasonable number of iterations can be found. There is always the chance that another combination of step size and iterations will results in a better outcome, as it is impossible to try out all possible combinations: a global optimal solution is not guaranteed.

An optimal solution is found when ∂u is smaller than a user defined tolerance value. But how to choose this tolerance? In this report the value for the tolerance (0.003) was taken from a continuous optimization example out of the book of Bryson (Bryson jr. 1999). The smaller the tolerance is chosen, the more difficult it will be to converge to an optimal solution. With the used continuous optimization scheme of Bryson it is not possible to check whether a global or local minimum has been reached. The only way to get an indication is by using different initial settings of the optimization algorithm and comparing the outcomes. This is time consuming and success is not guaranteed. When controlling only the inlet air flow, the optimization algorithm did not stop because the tolerance was met, but because the maximum number of iterations was exceeded (1000). Although improvements were obtained in comparison to piecewise linear optimization, an optimum was not reached although many different settings of the algorithm were used. Further research has to be performed to see if an optimum can be found.

During the research two versions of the software package Matlab have been used: versions 2009a and 2012a. During the computations there seemed to be a significant difference between the two versions. Version 2009a was up to 30% faster with the execution of the optimization code in comparison to version 2012a. Not only the execution time was different for the two versions, but also the outcomes were different when using the same code. These differences are caused by the different bit-versions and multi-thread capacities. Matlab version

2009a is 32-bit and version 2012a is 64-bit. With 64-bits it is possible to create and manipulated larger variables, and the addressable memory is significant larger. At the lowest level of operation, a 32-bit and 64-bit application may use CPU registers of differing widths, which result in slightly different answers due to round-off effects. There is also a difference in how both versions deal with multiple computer cores. The versions have different decision rules on which they decide how the divide the computational load over the available cores. All the results in this report are obtained with Matlab version 2009a.

During the research an attempt was made to solve the optimization problem using the software package Tomlab. Tomlab is an optimization environment in Matlab to solve all kinds of optimization problems. Tomlab has some advantages and some disadvantages in comparison to the software developed by Bryson (Bryson jr. 1999). An advantage of Tomlab is that the optimization problem can be formulated in a fast and easy way; only the cost function and the constraints have to be defined besides the process model. Tomlab is able to determine the problem type and selects automatically an appropriate solver to come to an optimal solution. It uses advanced solvers and is able to solve different kinds of optimization problems.

A disadvantage of Tomlab is that the solvers work with symbolic variables; so called Tomsyms. The use of Tomsyms prevents that logical statements like if-else, can be used in the code. Another disadvantage is that it is difficult to obtain the numeric value of a Tomsym variable for evaluation during execution of the code. The look-up table to determine the saturated moisture content of the air uses IF-statements, and Tomlab was not able to optimize the process without drastic modifications to the model or without a huge computational load. That is why Tomlab was not further used during this research and all optimizations were performed with the Bryson algorithm.

To determine the sensitivity of the optimal control trajectories to changes in the drying rate constant, a sensitivity analysis has been performed 100 times with a standard deviation of 10 % of the nominal value. The sensitivity analysis has only been performed in the situation where the inlet air temperature and flow are controlled. It is expected that a varying drying rate constant will have a bigger effect on the vitamin C retention ratio when only the temperature is controlled, as the distance between the state diagram and the vitamin C degradation area is smaller.

In the formulation of the energy efficiency constraint, a value of 1 is desired for the energy efficiency. An energy efficiency of 1 correspondents to an energy efficiency of 100 %. As presented before, it is possible to have an energy efficiency higher than 100 % when the product temperature is lower than the ambient temperature. The highest energy efficiency is reached when the inlet air temperature is at its minimum value and the moisture content of the air is at its saturated value. With these conditions the product temperature drops to 17.2 °C, which results in an energy efficiency of 128 %. This implies that the energy efficiency constraint should be changed such that the maximal energy efficiency of 128 % is desired. This adaptation has not been further researched in this thesis.

The costate trajectories show some remarkable events, and most of them are explained by the state and control trajectories. During this research, no clear explanation was found for all events and trajectories. Further research should be performed to come up with better explanations. There is also no interpretation assigned to the costate trajectories during this research. Because the costates have a link with the state and control trajectories, they maybe can be used to predict or to control the drying process. When uncertainty is introduced the costate trajectories may provide information which can be used to counter act the changes introduced by the uncertainty, such that the constrains of the process are met and the costs are minimized.

5 Conclusion

Jin presented piecewise linear and piecewise constant drying trajectories for drying broccoli stalks convectively, such that the vitamin C retention ratio and the energy efficiency remain high. Significant improvements were obtained in comparison to the traditional constant drying trajectories when controlling the inlet air temperature and flow of the dryer. To see if further improvements are possible, continuous optimization has been implemented during this thesis.

Before continuous optimization was implemented, the drying model used by Jin was corrected. In the original model the moisture content of the air could reach unrealistic high values, which resulted in a corresponding large temperature drop in the product. The adaptation to the drying model does not have a significant effect on the vitamin C retention ratio, because the moisture content of the air is only near its saturation point at the beginning of the drying process when the degradation rate constant is still small. The adaption has an effect on the energy efficiency, because the adaptation limits the temperature drop in the product due to evaporation, and the lower the product temperature will be in comparison to the ambient temperature, the higher the energy efficiency.

A continuous gradient based optimization scheme was implemented to control the drying process of broccoli stalks. In the situations, where only the inlet air temperature is controlled, or where the inlet air temperature and flow are controlled, improvements were obtained with continuous optimization in comparison to piecewise linear and constant optimization. When only the inlet air temperature was controlled, the vitamin C retention ratio improved from 35 to 38 % and the energy efficiency changed from 41 to 46 % in comparison to 4-stage piecewise linear control. In the situation where the inlet air temperature and flow were controlled, the vitamin C retention ratio improved from 45 to 75 % and the energy efficiency changed from 46 to 98 % in comparison to 4-stage piecewise linear control.

The drying rate constant was randomly changed 100 times with a standard deviation of 10 % around its nominal value. The sensitivity analysis showed that the drying rate constant has little effect on the vitamin C retention ratio, but a larger effect on the energy efficiency and the final product moisture content. The sensitivity analysis had been performed while using the inlet air temperature and flow as control variables. The sensitivity analysis resulted in mean vitamin C retention ratio of 74 % with a standard deviation of 0.63 %, a mean energy efficiency of 98 % with a standard deviation of 2.4 %, and a mean final product moisture content of 0.11 kg water / kg product with a standard deviation of 0.05 kg water / kg product. So the vitamin C retention ratio and the energy efficiency are not very sensitive to changes in the drying rate constant, while the product moisture content shows a lot of variation.

Jin already achieved superior results in comparison to the common constant control trajectories with piecewise linear and constant functions. This research showed that even better results can be achieved when continuous optimization is implemented. In the current time, where food quality is becoming more and more important and energy reduction is a big issue, continuous optimization can have a big impact on the drying process of food products.

The plotted costate trajectories show some remarkable events, and most of them are explained by examining to the state and control trajectories. For some events, a clear explanation is still missing. Further research should be performed to give a plausible explanation for all points and to see if the costate trajectories may be used to predict and to control the drying process in a more robust manner.

6 Literature

Bryson, A. E. and Y.-C. Ho (1975). Applied optimal control: optimization, estimation, and control, Taylor & Francis Group.

Bryson jr., A. E. (1999). Dynamic Optimization, Addison Wesley Longman.

Byers, T. and N. Guerrero (1995). "Epidemiologic evidence for vitamin C and vitamin E in cancer prevention." American Journal of Clinical Nutrition **62**(6 SUPPL.): 1385S-1392S.

Byers, T. and G. Perry (1992). "Dietary carotenes, vitamin C, and vitamin E as protective antioxidants in human cancers." Annual Review of Nutrition **12**: 139-159.

Eisma, J. (2010). Multi Cylinder Modelling of Broccoli Drying. Systems and Control Group. Wageningen, Wageningen University.

Henderson-Sellers, B. (1984). "A new formula for latent heat of vaporization of water as a function of temperature." Quarterly Journal of the Royal Meteorological Society **110**(466): 1186-1190.

Hussain, M. M. and I. Dincer (2003). "Two-dimensional heat and moisture transfer analysis of a cylindrical moist object subjected to drying: A finite-difference approach." International Journal of Heat and Mass Transfer **46**(21): 4033-4039.

Jin, X., R. van der Sman, G. van Straten, R. Boom and A. van Boxtel (2013). "ENERGY EFFICIENT DRYING STRATEGIES TO RETAIN NUTRITIONAL COMPONENTS IN BROCCOLI." Journal of Food Engineering.

Karim, O. and A. Adebowale (2009). "A dynamic method for kinetic model of ascorbic acid degradation during air dehydration of pretreated pineapple slices." International Food Research Journal **16**: 555-560.

Kemp, I. C. (2005). "Reducing dryer energy use by process integration and pinch analysis." Drying Technology **23**(9-11): 2089-2104.

Kudra, T. (2004). "Energy aspects in drying." Drying Technology **22**(5): 917-932.

Kudra, T. (2012). "Energy Performance of Convective Dryers." Drying Technology **30**(11-12): 1190-1198.

Law, C. L. and A. S. Mujumdar (2006). "8 Fluidized Bed Dryers."

Mishkin, M., I. Saguy and M. Karel (1984). "A Dynamic Test for Kinetic Models of Chemical Changes During Processing: Ascorbic Acid Degradation in Dehydration of Potatoes." Journal of Food Science **49**(5): 1267-1270.

Mulet, A., N. Sanjuán, J. Bon and S. Simal (1999). "Drying model for highly porous hemispherical bodies." **210**(2): 80-83.

Pontryagin, L., V. Boltyanskii and R. Gamkrelidze (1962). "The mathematical theory of optimal processes."

van Willigenburg, L. (2013). "Systems and Control Theory Part 2 ".

Verkerk, R., M. Schreiner, A. Krumbein, E. Ciska, B. Holst, I. Rowland, R. de Schrijver, M. Hansen, C. Gerhäuser, R. Mithen and M. Dekker (2009). "Glucosinolates in Brassica vegetables: The influence of the food supply chain on intake, bioavailability and human health." Molecular Nutrition and Food Research **53**(SUPPL. 2): 219-265.

von Stryk, O. and R. Bulirsch (1992). "Direct and indirect methods for trajectory optimization." Annals of Operations Research **37**(1): 357-373.

Voorrips, L. E., R. A. Goldbohm, G. Van Poppel, F. Sturmans, R. J. J. Hermus and P. A. Van Den Brandt (2000). "Vegetable and fruit consumption and risks of colon and rectal cancer in a prospective cohort study: The Netherlands Cohort Study on Diet and Cancer." American Journal of Epidemiology **152**(11): 1081-1092.